XI International Conference on Computational Plasticity. Fundamentals and Applications
COMPLAS XI
E. Oñate, D.R.J. Owen, D. Peric and B. Suárez (Eds)

MODELING OF DAMAGE IN SOFT BIOLOGICAL TISSUES AND APPLICATION TO ARTERIAL WALLS

Daniel Balzani*, Gerhard A. Holzapfel† and Sarah Brinkhues*

*Institute of Mechanics, University of Duisburg-Essen, Faculty of Engineering,
Universitätsstr. 15, 45117 Essen, Germany
e-mail: daniel.balzani@uni-due.de, www.uni-due.de/mechanika

†Graz University of Technology, Institute of Biomechanics, Center of Biomedical Engineering,
Kronesgasse 5-I, 8010 Graz, Austria
e-mail: holzapfel@tu-graz.at, www.biomech.tugraz.at
and
Royal Institute of Technology, Department of Solid Mechanics, School of Engineering Sciences,
Osquars Backe 1, 100 44 Stockholm, Sweden

Key words: Computational biomechanics, damage mechanics, arterial walls, softening behavior, soft biological tissues

Abstract. A new material model is proposed for the description of stress-softening observed in cyclic tension tests performed on soft biological tissues. The modeling framework is based on the concept of internal variables introducing a scalar-valued variable for the representation of fiber damage. Remanent strains in fiber direction can be represented as a result of microscopic damage of the fiber crosslinks. Particular internal variables are defined able to capture the nature of soft biological tissues that no damage occurs in the physiological loading domain. A specific model is adjusted to experimental data taking into account the supra-physiological loading regime. For the description of the physiological domain polyconvex functions are used which also take into account fiber dispersion in a phenomenological approach. The applicability of the model in numerical simulations is shown by a representative example where the damage distribution in an arterial cross-section is analyzed.

1 INTRODUCTION

As a result of hypertension, overweight, rich alimentation, smoking, diabetes and stress, biochemical and mechanical degenerative processes in arterial walls are followed by a lumen reduction referred to as stenosis. In severe cases such stenosis may result in heart attacks, smoker's legs or in strokes. To prevent such complications one frequently used method of treatment is balloon dilatation accompanied by the implantation of a stent.

Thereby, a balloon catheter is inserted into the affected artery and dilated with an internal pressure increase. After removing the balloon the luminal area remains enlarged. During this procedure microscopic damage is induced in the vessel wall which is partly responsible for the treatment success since it results in increased strains when unloading to the state of physiological blood pressure again. Within the clinical context these effects are referred to as controlled vessel injury, see, e.g., [5]. In order to improve insight into the complex biomechanical processes during therapeutical interventions such as angioplasty and for the optimization of treatment methods, the modeling of arterial tissues and related computer simulations are subject of current research.

Most experimental approaches dealing with the measurement of mechanical properties of soft biological tissues are related to the analysis of loading within the physiological domain. With respect to degenerative processes occurring during angioplasty especially supra-physiological (therapeutical) loadings are required. These load levels are characterized by loading conditions significantly higher than those that occur under normal (physiological) conditions. In [19] first layer-specific experiments are performed under supra-physiological conditions. In such experiments a pronounced softening hysteresis is observed with respect to the stress-strain response. For the description of isotropic softening there exist various models. One of the first representations of damage at large strains is introduced in [20]. In order to describe damage, showing a saturating behavior during repeated un- and reloading cycles for fixed maximum load levels, [13] introduced a suitable model. An alternative phenomenological form of describing damage mechanisms is linked with the notion of pseudo-elasticity. Thereby, the main idea is that different loading branches are described by different strain-energy functions. As one of the first works in this context one should mention [15]. With respect to soft biological tissues a practical approach avoiding the usage of damage tensors is given in [17], where the anisotropic damage can be described by scalar-valued variables. The model by [16] uses scalar-valued variables as well and considers a stochastic framework on the basis of the wavy structure of the collagen fibers. A model for the preconditioning of soft biological tissues and the anisotropic Mullins effect is proposed in [7]. Another recent approach provides the description of remanent strains after overstretch in the framework of finite plasticity based on the assumption of remaining deformations at the micro-scale of the fibers, see [9]. A particular damage behavior for the matrix material is taken into account in e.g. [14] or [4]. These two contributions are formulated in terms of the continuum damage mechanics, where the existence of an effective (ficticiously undamaged) strain energy function is postulated. Since this function is associated to the physiological regime, where the response of soft biological tissues is hyperelastic, a polyconvex function should be used because then the existence of minimizers of underlying variational problems is guaranteed if additionally coercivity is ensured. In addition to that, quasiconvexity and material stability are automatically fulfilled, cf. [18], where the first transversely isotropic and orthotropic polyconvex functions are introduced. In [10] a first polyconvex model for arterial tissues is proposed as an exponential function of the fourth mixed invariant

of the right Cauchy-Green tensor and the structural tensor characterizing the material symmetries. Further polyconvex models able to describe soft biological tissues which are a priori stress-free in the (undeformed) reference configuration are proposed in, e.g., [1] or [6].
Here, we focus on the construction of a new model able to describe the complex softening hysteresis observed in experiments of soft biological tissues. The model is formulated in terms of the continuum damage mechanics and reflects the anisotropic character of the material. In addition to that, a rather low number of material parameters with physical interpretability is introduced keeping the proposed model applicable. Please note that full details regarding the model and numerical examples can be found in the original paper [3].

2 CONTINUUM MECHANICAL FRAMEWORK

In the reference configuration the body of interest is denoted by $\mathcal{B} \subset \mathbb{R}^3$ and parameterized in $\boldsymbol{X}$; in the deformed configuration it is denoted by $\mathcal{S} \subset \mathbb{R}^3$ and parameterized in $\boldsymbol{x}$. The nonlinear deformation map $\boldsymbol{\varphi}_t : \mathcal{B} \to \mathcal{S}$ at time $t \in \mathbb{R}_+$ maps points $\boldsymbol{X} \in \mathcal{B}$ onto points $\boldsymbol{x} \in \mathcal{S}$. The deformation gradient $\boldsymbol{F}$ and the right Cauchy–Green tensor $\boldsymbol{C}$ are defined by

$$\boldsymbol{F}(\boldsymbol{X}) := \nabla \boldsymbol{\varphi}_t(\boldsymbol{X}) \quad \text{and} \quad \boldsymbol{C} := \boldsymbol{F}^T \boldsymbol{F} \,, \tag{1}$$

with the Jacobian $J := \det \boldsymbol{F} > 0$. In case of hyperelastic materials we postulate the existence of a strain-energy function ψ, defined per unit reference volume. In order to obtain constitutive equations which satisfy *a priori* the principle of material objectivity, the functional dependency $\psi := \psi(\boldsymbol{C})$ is taken into account. Then we compute the second Piola–Kirchhoff stresses and the Cauchy stresses by

$$\boldsymbol{S} = 2\partial_C \psi \quad \text{and} \quad \boldsymbol{\sigma} = J^{-1} \boldsymbol{F} \boldsymbol{S} \boldsymbol{F}^T \,, \tag{2}$$

respectively. A suitable framework for the description of anisotropic materials is the concept of structural tensors. Therein, an additional argument tensor, the structural tensor, is defined such that it reflects the symmetry group of the considered material. We concentrate on fiber-reinforced materials, hence, we restrict ourselves to the cases of transverse isotropy and to materials which can be characterized by a given number of non-orthogonal preferred directions. In these cases we are able to express the material symmetry of the considered body by a set of second-order structural tensors

$$\boldsymbol{M}_{(a)} := \boldsymbol{A}_{(a)} \otimes \boldsymbol{A}_{(a)} \quad \text{with} \quad a = 1...n_a \,, \tag{3}$$

where n_a is the number of fiber directions. For the construction of specific constitutive equations we focus on a coordinate-invariant formulation, thus, the invariants of the deformation tensor and of the structural tensors are required. The explicit expressions for the principle invariants of the right Cauchy–Green tensor are given by

$$I_1 := \operatorname{trace} \boldsymbol{C}, \quad I_2 := \operatorname{trace}[\operatorname{Cof} \boldsymbol{C}], \quad I_3 := \det \boldsymbol{C} \,. \tag{4}$$

Let $\boldsymbol{M}_{(a)}$ be of rank one and let us assume the normalization condition $||\boldsymbol{M}_{(a)}|| = 1$ due to $|\boldsymbol{A}_{(a)}| = 1$, then the additional invariants, the mixed invariants, are

$$J_4^{(a)} := \text{trace}[\boldsymbol{C}\boldsymbol{M}_{(a)}], \quad J_5^{(a)} := \text{trace}[\boldsymbol{C}^2\boldsymbol{M}_{(a)}] \,. \tag{5}$$

For the construction of constitutive equations we obtain the possible polynominal basis $\mathcal{P}_1 := \{I_1, I_2, I_3, J_4^{(a)}, J_5^{(a)}\}$.

3 DAMAGE MODEL FOR SOFT BIOLOGICAL TISSUES

In arterial walls the tissues are basically composed of an isotropic ground substance and mainly two embedded fiber families, which are typically arranged cross-wise helically. This fiber-reinforcement can be taken into account by consideration of a strain energy function of the type

$$\psi(I_1, I_2, I_3, J_4^{(a)}, J_5^{(a)}) := \psi^{vol}(I_3) + \psi^{iso}(I_1, I_2, I_3) + \sum_{a=1}^{2} \psi_{(a)}^{ti}(I_1, I_3, J_4^{(a)}, J_5^{(a)}) \,. \tag{6}$$

The energy associated to the isotropic ground substance is represented by ψ^{iso} whereas the fiber energy is denoted by $\psi_{(a)}^{ti}$. A weak interaction between the individual fiber families is assumed and therefore the orthogonal response of the material is approximated by the superposition of two transversely isotropic energies. The energy ψ^{vol} is a penalty function accounting for the incompressibility constraint. Here, it is assumed that the ground-substance is able to undergo significantly higher deformations before a dissipative behavior is observed and therefore no damage is taken into account in the matrix. The associated strain energy function is chosen as

$$\psi^{iso} = c_1 \left(\frac{I_1}{I_3^{1/3}} - 3 \right) , \tag{7}$$

where $c_1 > 0$ is a stress-like material parameter. This function leads to an almost linear stress-strain relationship which can be experimentally substantiated.
For the description of the damage-induced softening observed in experiments the main damage evolution is assumed to be in the fibers since these are the main load-bearing elements. Therefore, the transversely isotropic part is decomposed into the effective (ficticiously undamaged) hyperelastic strain energy $\psi_{(a)}^0$ and a reduction term $(1 - D_{(a)})$ with $D \in [0, 1[$ accounting for the microscopic damage evolution. In order to consider remanent strains in the fibers when unloading the material a further decomposition into an external and an internal function m and P is taken into account, respectively. Then we obtain

$$\psi_{(a)}^{ti} := m(P(\boldsymbol{C}, D_{(a)})) \quad \text{with} \quad P = (1 - D_{(a)})\, \psi_{(a)}^{ti,0} - c \,, \tag{8}$$

wherein the constant value c represents the value of the effective energy in the reference configuration. For the external and effective strain energy function we choose

$$m(P_{(a)}) = \frac{k_1}{2k_2}\left\{\exp\left(k_2\langle P_{(a)}\rangle^2\right) - 1\right\}\,, \quad \psi_{(a)}^{ti,0} = \kappa\, I_1 + (1-3\,\kappa) J_4^{(a)}\,, \quad c = 1 \tag{9}$$

such that for the undamaged case ($D = 0$) the well-known strain energy function [10] together with the fiber dispersion approach introduced in [8] is obtained. This approach is incorporated in order to account for distributed fiber orientations, which is controlled by adjusting the parameter $\kappa \in [0, 1/3]$. If $\kappa = 0$ then a perfectly transversely isotropically distributed orientation is obtained. Please note that the Macauley bracket $\langle(\bullet)\rangle = \frac{1}{2}[(\bullet) + |(\bullet)|]$ in $(9)_1$ filters out positive values. Preliminary mechanical experiments of cyclically overstretched soft biological tissues show that if the maximum load level is fixed in a cyclic tension test, then the stress hysteresis converges to a "saturated" response curve. This behavior has to be modeled by an appropriate choice of the damage function D, which is assumed to depend on the fictitiously undamaged (effective) energy $\psi_{(a)}^{ti,0}$, cf. [2], such that evolution of damage is activated in the loading and reloading processes. This can be achieved by defining the internal variable

$$\beta_{(a)} := \left\langle \tilde{\beta}_{(a)} - \tilde{\beta}_{(a)}^{ini} \right\rangle \quad \text{with} \quad \tilde{\beta}_{(a)} = \int_0^t \left\langle \dot{\psi}_{(a)}^{ti,0}(s) \right\rangle ds\,, \tag{10}$$

with $\tilde{\beta}_{(a)}^{ini}$ being the internal variable at an initial damage state in order to make sure that the damage evolution starts when entering the supra-physiological domain. Clearly, $\tilde{\beta}_{(a)}^{ini}$ is the value of $\tilde{\beta}_{(a)}$ at each material point reached for the situation where the damage evolution starts. In arterial walls this should be the case when the upper edge of "normal" blood pressure is attained. The time associated to the loading history is denoted by $s \in \mathbb{R}^+$; $t \in \mathbb{R}^+$ defines the actual loading situation. Then the internal variable (10) enters the damage function

$$D_{(a)}(\beta) = D_{s,(a)}\left[1 - \exp\left(\frac{\ln(1-r_s)}{\beta_s}\,\beta_{(a)}\right)\right] \quad \text{with} \quad D_{s,(a)} \in [0,1[\,,\ r_s \in [0,1[\,,\ \beta_s > 0\,, \tag{11}$$

cf. [12]. Herein, the only material parameter β_s is the value of the internal variable β which is reached at a certain fraction r_s of the maximal damage value $D_{s,(a)}$ for a fixed maximum load level. We consider a fraction of $r_s = 0.99$ and thus, β_s represents the value of internal variable at a damage value which can be interpreted as saturated. The response of the damage function (11) converges to a maximum value of damage $D_{s,(a)}$, which is in turn not a specified number but rather a function increasing the maximally reachable damage value for increased maximum load levels. For convenience we consider the same type of function and define

$$D_{s,(a)}(\gamma_{(a)}) = D_\infty\left[1 - \exp\left(\frac{\ln(1-r_\infty)}{\gamma_\infty}\gamma_{(a)}\right)\right] \quad \text{with} \quad D_\infty \in [0,1[\,,\ r_\infty \in [0,1[\,,\ \gamma_\infty > 0\,. \tag{12}$$

The parameter γ_∞ represents the value of the internal variable γ reached at the fraction $r_\infty = 0.99$ of D_∞; D_∞ denotes a predefined converging limit for the overall damage value. In order to take into account that $D_{s,(a)}(\gamma)$ remains unaltered for cyclic processes under fixed maximum load levels we consider the internal variable

$$\gamma_{(a)} = \max_{s\in[0,t]} \left\langle \psi^{ti,0}_{(a)}(s) - \psi^{ti,0}_{(a),ini} \right\rangle , \tag{13}$$

which is defined as the maximum value of effective energy reached up to the actual state. Herein, $\psi^{ti,0}_{ini,(a)}$ denotes the effective strain energy at an initial damage state obtained at the limit of the physiological domain. This expression leads to the saturation criterion

$$\phi_{(a)} := \left\langle \psi^{ti,0}_{(a)} - \psi^{ti,0}_{(a),ini} \right\rangle - \gamma_{(a)} \leq 0 \, . \tag{14}$$

Since D_∞ will be usually a number close to 1, the proposed damage model gets along with the two material parameters β_s and γ_∞, which have to be adjusted to experimental data.
The second Piola-Kirchhoff stresses are then computed from

$$\boldsymbol{S} = 2\,\frac{\partial \psi}{\partial \boldsymbol{C}} = \boldsymbol{S}^{vol} + \boldsymbol{S}^{iso} + \sum_{a=1}^{2} \boldsymbol{S}^{ti}_{(a)} \, , \tag{15}$$

with the individual abbreviations

$$\boldsymbol{S}^{vol} = 2\,\frac{\partial \psi^{vol}}{\partial \boldsymbol{C}} \, , \; \boldsymbol{S}^{iso} = 2\,\frac{\partial \psi^{iso}}{\partial \boldsymbol{C}} \, , \; \boldsymbol{S}^{ti}_{(a)} = m'(1-D_{(a)})\,\boldsymbol{S}^{ti,0}_{(a)} \quad \text{and} \quad \boldsymbol{S}^{ti,0}_{(a)} = 2\,\frac{\partial \psi^{ti,0}_{(a)}}{\partial \boldsymbol{C}} \, . \tag{16}$$

It is emphasized that in the physiological (hyperelastic) regime where $D_{(a)} = 0$ the strain energy function is polyconvex and coercive and ensures therefore the existence of minimizers and material stability.

4 NUMERICAL EXAMPLES

In this section numerical examples are provided. First, the proposed model is adjusted to uniaxial tension tests performed with test stripes taken from the media of a human carotid artery in order to show that the model is able to capture the mechanical behavior of arterial tissues. Second, a circumferential overstretch of an atherosclerotic artery is simulated in order to analyze the distribution of damage through the arterial wall.

4.1 ADJUSTMENT TO EXPERIMENTAL DATA

Uniaxial tension tests are performed on two test stripes taken from the media of a human carotid artery, where one stripe is extended in circumferential and the other one

	c_1 [kPa]	k_1 [kPa]	k_2 [-]	α_1 [kPa]	α_2 [-]	κ [-]	β_f [°]	D_∞ [kPa]	γ_∞ [kPa]	β_s [-]
physiological	6.56	1482.38	564.81	-	-	0.16	37.03			
supra-physiological	7.50	1266.57	400.0	-	-	0.19	35.05	0.99	6.71	1e-8

Table 1: Material parameters of the proposed model for the media of a human carotid artery in the purely physiological and in the supra-physiological loading domain.

in axial direction. The proposed model is adjusted to the experimental data by minimizing the least-square function

$$\bar{r}(\boldsymbol{\alpha}) = \sum_{e=1}^{n_e} \sqrt{\frac{1}{n_{mp}} \sum_{m=1}^{n_{mp}} \left(\frac{\sigma_{exp}(\lambda_1^{(m)}) - \sigma_{comp}(\lambda_1^{(m)}, \boldsymbol{\alpha})}{\max[\sigma_{exp}]} \right)^2}, \tag{17}$$

wherein σ_{exp} and σ_{comp} denote the experimentally measured and modeled Cauchy-stresses, respectively; $\lambda_1 = F_{11}$ denotes the stretch in the tension direction which coincides with the x_1-direction. Two experiments, i.e. tension in circumferential and axial direction ($n_\mathrm{e} = 2$) are considered and a number of n_{mp} measuring points are taken into account. The material parameters are arranged in the vector $\boldsymbol{\alpha}$ and identified by minimizing $\bar{r}$. In order to incorporate incompressibility the penalty term $\psi^{vol} = p(I_3 - 1)$ is included in the strain energy function, where p can be interpreted as a pressure-like Lagrange multiplier. The angle between the fiber orientation and the circumferential direction is treated as a fitting parameter and is defined to be β_f. In order to weight the two experiments in a representative manner the differences are normalized by the maximal values of the experimental stresses reached for the actual loading cycle. For the minimization problem sequential quadratic programming is applied.

In the first instance, only the hyperelastic, physiological regime is considered. Here, the number of measuring points is $n_{mp} = 49$ for the axial and $n_{mp} = 43$ for the circumferential tension test. The resulting hyperelastic material parameters are listed in the first row of Table 1. Fig. 1a shows the corresponding hyperelastic stress-strain response of the model compared with experimental data. As can be seen in this figure the model lead to an accurate match of the experimental data. Furthermore, the model response is adjusted to experimental data for significantly increased loadings such that the supra-physiological domain can be analyzed. For this purpose cyclic uniaxial tension tests in circumferential and axial direction are considered. The results of the experiments are shown in Fig. 1b. A strong anisotropy as well as a pronounced softening hysteresis is observed.

For the least-squares fit the hyperelastic parameters given in Table 1 (physiological) serve as estimators for the definition of suitable bounds for the hyperelastic parameters. Then, the hyperelastic as well as the damage parameters are adjusted. Due to this procedure, the fit provides the parameters given in the second row of Table 1. Fig. 1c shows the resulting response of the proposed model. We observe a good qualitative and quantitative correlation with the experiments.

4.2 NUMERICAL SIMULATION OF ATHEROSCLEROTIC ARTERY

In the following a numerical example for the anisotropic damage model described above is given by a numerical simulation of an atherosclerotic arterial wall. A stenosis caused by atherosclerosis is mostly treated by a balloon-angioplasty in combination with stenting. In this context, a high internal (supra-physiological) pressure acts on the arterial wall during inflating an inserted dilatation-catheter. The purpose of this section is to simulate such an arterial overexpansion in a two-dimensional approximation which basically enables the investigation of the influence due to the circumferential overstretch.
Therefore, a two-dimensional geometrical model with an average diameter of approximately one centimeter is used and computed with 6048 triangular elements with quadratic ansatz functions. The model is constructed based on hrMRI (high resolution magnetic resonance imaging). The considered cross-section is shown in Fig. 2a, where the discretization and the particular components are depicted.

The components of the artery are identified by hrMRI examination and histological analysis, namely the nondiseased intima, fibrous cap (Ifc), i.e. the fibrotic part at the luminal border, fibrotic intima at the medial border, calcification (Ic), lipid pool (Ilp), nondiseased media, diseased fibrotic media and adventitia (Adv), cf. [11]. For the numerical investigation the nondiseased intima with its less significant mechanical behavior is neglected and the fibrotic intima at the medial border and the diseased fibrotic media are combined to fibrotic media (Mf). The parameters for the media originate from Section 4.1 and the parameters for the adventitia are adjusted analogously to cyclic experiments such that the parameters given in Table 2 (Adv) are obtained. Unfortunately, for the fibrous cap and the fibrotic media no data is available for the supra-physiological regime and therefore the model is adjusted to the physiological data given in [11] and the same damage parameter identified for the media are taken. The lipid pool is assumed to be a butterlike, incompressible fluid not able to sustain shear stress. For the nearly rigid calcificated regions an average Youngs Modulus of 12(+-4.7) MPa is regarded. No damage is considered within the calcification and the lipid regions, because here dam-

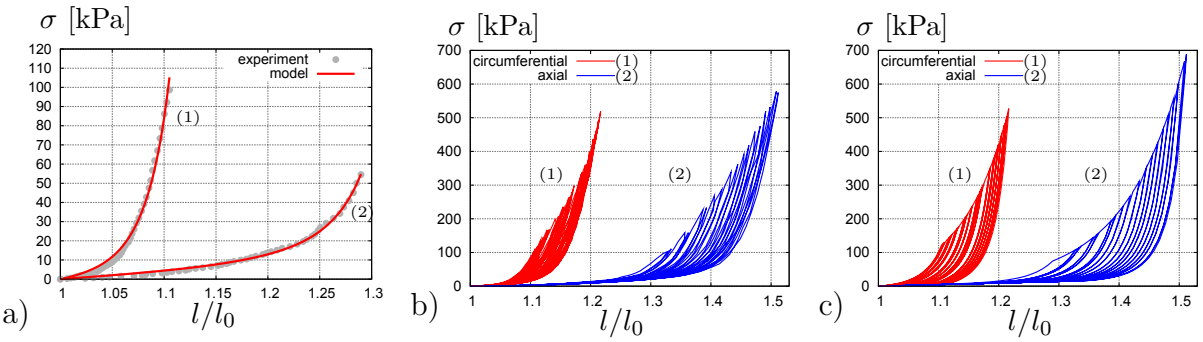

Figure 1: Uniaxial tension tests of the media of a human carotid artery in circumferential (1) and axial (2) directions: a) Comparison of the constitutive model response with experimental data in the physiological range; Cyclic uniaxial tension tests: b) experimental data and c) results of the constitutive model.

age plays a minor role. An overview of all parameters are listed in Table 2. For the nondiseaed and fibrotic media, the adventitia and the fibrous cap, which sustain damage evolution, the parameters $r_s = r_\infty = 0.99$ are taken into account. In order to enforce the incompressibility constraint, the penalty function $\psi^{vol} = \varepsilon_1 \left(I_3^{\varepsilon_2} + I_3^{-\varepsilon_2} - 2\right)$ is used, where the parameters ε_1 and ε_2 are chosen such that $\det \boldsymbol{F} = 1 \pm 1\%$ in the numerical simulation. For the simulation, first an internal pressure of 24.0 kPa ($\hat{=}$ 180.0 mmHg) representing the upper edge of the physiological regime and simultaneously an axial prestretch of 2% is applied. This situation is defined to be the initial damage state meaning that damage evolution starts after a pressure higher than 24.0 kPa. In a further step the internal pressure is increased up to 150.0 kPa ($\hat{=}$ 1125.0 mmHg) in order to simulate the overexpansion of the artery. After that the internal pressure is decreased till reaching a pressure of $p = 24.0$ kPa again, i.e. the natural state after a balloon-angioplasty. Here, no circumferential eigenstrains are considered because their order of magnitude is relatively small compared to the stresses resulting from the overstretch and their influence on the situation after the overstretch is assumed to be negligible. In Fig. 2b the distribution of the normalized damage variable $D_{(1)}/\max D_{(1)}$ is depicted at an internal blood pressure of 180 mmHg after the overstretch. A damage concentration in the healthy part of the media and the fibrous cap are observed. In addition to that the remaining strains under physiological blood pressure are significant by comparing the cross-section area A of the lumen before ($A_0 \approx 0.11$ cm^2) and after ($A \approx 0.17$ cm^2) the overexpansion. The resulting increase of the blood lumen due to the overstretch is $0.17/0.11 \approx 1.5$.
Remark: this simulation of an arterial wall can only be interpreted as an illustration that the proposed model provided in this contribution is able to be implemented in finite-element simulations. Although the qualitative distribution of damage may be reasonable the quantitative results are not necessarily realistic due to the lack of experimental data

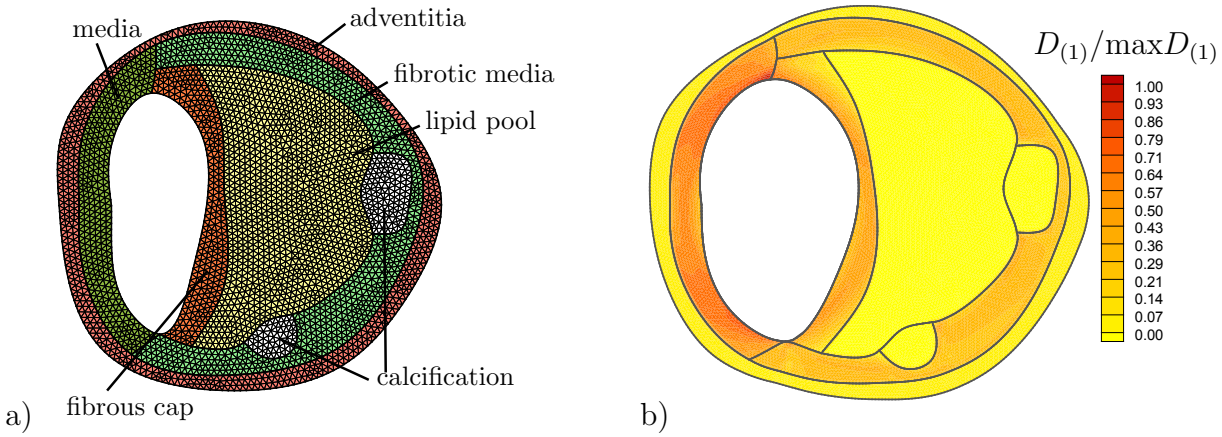

Figure 2: a) Cross section of the arterial model discretized with 6048 quadratic triangular finite elements; the components are: adventitia (Adv), nondiseased media, fibrotic media (Mf), fibrous cap (Ifc), lipid pool (Ilp), calcification (Ic); b) normalized damage variable $D_{(1)}/\max D_{(1)}$ with $\max D_{(1)} = 0.1048$ of a loaded artery after overexpansion at an internal pressure of $p = 24$ kPa (180 mmHg).

	c_1 [kPa]	k_1 [kPa]	k_2 [-]	κ [-]	β_f [°]	D_∞ [kPa]	γ_∞ [kPa]	β_s [-]
Adv	4.0	1640.23	115.63	0.097	45.60	0.99	10.84	7.36
Mf	21.12	1951.48	925.37	0.095	25.55	0.99	6.52	0.37
Ifc	24.12	4778.44	1023.59	0.12	53.18	0.99	6.52	0.37
Ic	2250.0	–	–	–	–	–	–	–
Ilp	2.5	–	–	–	–	–	–	–

Table 2: Hyperelastic and damage parameters of the other components.

and the two-dimensional approximation of the three-dimensional artery.

5 CONCLUSION

An anisotropic damage model for soft biological tissues was presented able to describe stress-softening hysteresis and remanent strains in the collagen fibers after unloading. A specific constitutive model was given and by defining suitable internal variables an undamaged physiological loading regime could be taken into account. The resulting strain energy function is polyconvex and coercive in the physiological (hyperelastic) regime and guarantees therefore the existence of minimizers of variational problems. The proposed model has been adjusted to cyclic uniaxial tension tests of the media and adventitia of a human carotid artery and an accurate matching was observed. Furthermore, a circumferential overstretch of an atherosclerotic artery was simulated in order to show the performance of the proposed model in finite element calculations.

ACKNOWLEDGEMENT: The authors greatly appreciate the Deutsche Forschungsgemeinschaft (DFG) for the financial support under the research grant BA 2823/5-1.

REFERENCES

[1] Balzani, D., Neff, P., Schröder, J. and Holzapfel, G.A., A polyconvex framework for soft biological tissues. Adjustment to experimental data, *International Journal of Solids and Structures* (2006) **43/20**:6052–6070.

[2] Balzani, D., Polyconvex anisotropic energies and modeling of damage applied to arterial walls, PhD-thesis, *Report No 2 of the Institute of Mechanics at the University of Duisburg-Essen* (2006), Verlag Glückauf Essen, ISBN 3-7739-6019-0.

[3] Balzani, D., Brinkhues, S. and Holzapfel, G.A., Constitutive framework for the modeling of damage in soft biological tissues (2011), submitted

[4] Calvo, B., Peña, E., Martínez, M.A. and Doblaré, M., An uncoupled directional damage model for fibered biological soft tissues, *International Journal for Numerical Methods in Engineering* (2007) **69**:2036–2057.

[5] Castaneda-Zuniga, W, Pathophysiology of transluminal angioplasty. *Improvement of myocardial perfusion* (Eds.: Meyer, J. and Erberl, R. and Rupprecht, H. J.), Martinus Nijhof (publisher), Boston (1985).

[6] Ehret, A. and Itskov, M., A Polyconvex Hyperelastic Model for Fiber-Reinforced Materials in Application to Soft Tisues, *Journal of the Mechanics and Physics of Solids* (2007) **42**:8853–9963.

[7] Ehret, A. and Itskov, M., Modeling of Anisotropic Softening Phenomena: Application to Soft Biological Tissues, *International Journal of Plasticity* (2009) **25**:901–919.

[8] Gasser, T.C., Ogden, R.W. and Holzapfel, G.A., Hyperelastic modelling of arterial layers with distributed collagen fibre orientations, *Journal of the Royal Society Interface* (2006) **3**:15–35.

[9] Gasser, T.C. and Holzapfel, G.A., Finite element modeling of balloon angioplasty by considering overstretch of remnant non-diseased tissues in lesions, *Computational Mechanics* (2007) **40**:47–60.

[10] Holzapfel, G. A., Gasser, T.C. and Ogden, R.W., A new constitutive framework for arterial wall mechanics and a comparative study of material models, *Journal of Elasticity* (2000) **61**:1–48.

[11] Holzapfel, G.A., Sommer, G. and Regitnig, P., Anisotropic Mechanical Properties of Tissue Components in Human Atherosclerotic Plaques, *Journal of Biomechanical Engineering* (2004) **126**:657–665.

[12] Miehe, C., Discontinuous and continuous damage evolution in Ogden-type large-strain elastic materials, *European Journal of Mechanics, A/Solids* (1995) **14**:697–720.

[13] Miehe, C. and Keck, J., Superimposed finite elasticviscoelasticplastoelastic stress response with damage in filled rubbery polymers. Experiments, modelling and algorithmic implementation, *Journal of the Mechanics and Physics of Solids* (2000) **48**:323–365.

[14] Natali, A.N., Pavan, P.G., Carniel, E.L. and Dorow, C., A transversally isotropic elasto-damage constitutive model for the periodontal ligament, *Computer Methods in Biomechanics and Biomedical Engineering* (2003) **6**:329–336.

[15] Ogden, R.W. and Roxburgh, D.G., An energy-based model of the Mullins effect, *Proceedings of the First European Conference on Constitutive Models*, (Eds.: Al Dorfmann and Alan Muhr), A. A. Balkema (publisher), Rotterdam, Brookfield (1999) 23–28.

[16] Rodríguez, J.F., Cacho, F., Bea, J.A., and Doblaré, M., A stochastic-structurally based three dimensional finite-strain damage model for fibrous soft tissue, *Journal of the Mechanics and Physics of Solids* (2006) **54**:864–886.

[17] Schröder, J., Balzani, D. and Gross, D., Aspects of modeling and computer simulation of soft tissues: applications to arterial walls, *Materialwissenschaft und Werkstofftechnik* (2005) **36/12**:795–801.

[18] Schröder, J. and Neff, P., Invariant formulation of hyperelastic transverse isotropy based on polyconvex free energy functions, *International Journal of Solids and Structures* (2003) **40**:401–445.

[19] Schulze-Bauer, C.A.J., Regitnig, P., and Holzapfel G.A., Mechanics of the human femoral adventitia including the high-pressure response, *American Journal of Physiology - Heart and Circulatory Physiology* (2002) **282**:H2427–H2440.

[20] Simo, J.C., On a fully three-dimensional finite-strain viscoelastic damage model: formulation and computational aspects, *Computer Methods in Applied Mechanics and Engineering* (1987) **60**:153–173.